Available online at www.sciencedirect.com
ScienceDirect
Inorganica Chimica Acta 360 (2007) 170–178
Inorganica Chimica Acta
www.elsevier.com/locate/ica

Engineered Si(100) surfaces for the gas-phase anchoring of metal β-diketonate complexes

Guglielmo G. Condorelli *, Alessandro Motta, Cedric Bedoya, Alessandro Di Mauro, Giovanna Pellegrino, Emanuele Smecca

Dipartimento di Scienze Chimiche, Università di Catania and INSTM UdR di Catania, V.le A. Doria 6, 95125 Catania, Italy

Received 16 June 2006; received in revised form 27 July 2006; accepted 27 July 2006
Available online 9 August 2006

Inorganic Chemistry – The Next Generation.

Abstract

A synthetic strategy for the covalent anchoring of nickel β-diketonate complexes on Si(100) has been examined. Engineered Si(100) surfaces were prepared by the Si-grafting of 10-undecylenic acid methyl ester followed by hydrolysis of the ester to free the carboxylic functions suited for the anchoring of the Ni complex. Bis(pentane-2,4-dionate)Ni(II) was bonded to the functionalized surface from the gas phase by the exchange of the acetylacetonate ligand with the grafted acid. The surface density of the anchored Ni complex was controlled by tuning the surface concentration of carboxylic groups adopting a mixed monolayer of undecylenic acid and 1-decene used as a spectator spacer. The nickel decorated silicon surfaces were characterized by attenuate total reflectance infrared absorption spectroscopy (ATR-IRAS) and angle resolved X-ray photoelectron spectroscopy (AR-XPS).

Keywords: SAM; Functionalized surfaces; Silicon surface; Nickel compounds; Acetylacetonates; X-ray photoelectron spectroscopy

1. Introduction

The ability to control the chemical and structural properties of surfaces is crucial for new technological advancements in a wide range of technological fields from microelectronics [1] and chemical sensing [2–6] to bio- [7] and nano-technologies [8,9]. In particular, the preparation of hybrid inorganic/organic systems plays a crucial role in the tailoring of suitable surfaces for applicative materials and devices such as catalysts [10], biosensors [11,12], nanosystems [13,14], and drug delivery [15]. Direct grafting of transition metal β-diketonates (e.g. M^{n+} = Ni, Co, Fe, Cr,) on inorganic surfaces such as silica, alumina, and zeolites is matter of great interest for interface processes in gas chromatography [16] and in catalysis [17–21]. On the other hand, self-assembled monolayers (SAMs) derived through the chemisorption of 'host' organic monolayers on various surfaces have allowed innovative synthetic routes since a large variety of molecules can be attached to organic functionalities using coordination chemistry. In this context, the insertion of metal-organic compounds into organized assemblies has created a growing interest due to its potential applications [22–29]. Immersion of carboxyl-terminated SAMs hosted on gold substrates into aqueous solutions of metal salts (e.g. Cu, Co, Cr, Os) leads to metal cation chemisorption at the surface with complex formation [30]. However, this wet chemical functionalization is limited by the poor efficiency in obtaining conformal coverage on 3D structures. The possibility of making gas phase deposition of metal onto gold supported SAM has been also investigated [31–33]. Despite the large amount of work devoted to the study of gold based SAM, much less effort has been

* Corresponding author. Fax: +39 095580138.
E-mail address: guidocon@unict.it (G.G. Condorelli).

0020-1693/$ - see front matter © 2006 Elsevier B.V. All rights reserved.
doi:10.1016/j.ica.2006.07.079

devoted to possible insertion of metal-organic compounds on silicon hosted SAMs. Prospects of molecular devices find the most promising architecture in hybrid systems in which a dense array of molecular devices is hosted on a surface of technological importance such as Si(1 0 0) [34].

In the present paper, we report the controlled anchoring from gas phase of bis(pentane-2,4-dionate)nickel(II) (thereafter $Ni(acac)_2$) on engineered Si(1 0 0) surfaces. The β-diketonate anchoring required first the covalent grafting of 10-undecylenic acid onto Si surfaces followed by the anchoring of the metal β-diketonate on the –COOH terminations. Among the various covalent bonding modes of organic molecules on silicon surfaces, the present work focuses on the hydrosilylation reaction of alkenes on H-terminated Si, since this approach appears the best suited for a large number of potential applications [35]. It is well documented [35,36] that the hydrosilylation of multiple bonds leads to the formation of robust Si–C bonds between the surface and the organic molecules.

In particular, mixed monolayers of undecylenic acid and 1-decene as the spectator spacer were anchored on silicon in order to control the surface density of the functional carboxylic groups and, in turn, the amount of anchored nickel. A similar strategy was proved capable of controlling the surface density of Mn-based magnetic clusters anchored by liquid routes [37]. The resulting nickel decorated silicon surfaces were characterized using attenuate total reflectance infrared absorption spectroscopy (ATR-IRAS) and angle resolved X-ray photoelectron spectroscopy (AR-XPS). The latter technique is an ideal tool for the characterization of the nanometric layer as well as to probe the elemental depth distribution and the bonding states.

2. Experimental

All chemicals, unless otherwise noted, were commercially available and used as received. Solvents for substrate cleaning were distilled. The 1-decene for monolayer preparation was distilled under reduced pressure over Na metal.

The 10-undecylenic acid methyl ester was synthesized according to the method reported by Sieval et al. [35a]. A mixture of 10-undecylenic acid (10 g, 54 mmol), 65 ml of methanol, and 0.14 ml of sulfuric acid was refluxed for 3 h. The methanol excess was removed in vacuum, and the resulting material was dissolved in ether. The product was distilled under vacuum to obtain a transparent liquid.

^{1}H NMR (500 MHz, $CDCl_3$, 25 °C, TMS): $\delta = 5.83$–5.78 (m, 1H), $\delta = 5.00$–4.91 (m, 2H), $\delta = 3.66$ (s, 3H), $\delta = 3.31$–2.84 (m, 2H), $\delta = 2.06$–2.01 (m, 2H), $\delta = 1.63$–1.9 (m, 2H), $\delta = 1.38$–1.29 (m, 10H).

Diluted self-assembled organic monolayers were prepared by Si-grafting of mixtures of 10-undecylenic acid methyl ester and 1-decene with different mole ratios: χ_{ester} (soln) = 0.0, 0.1, 0.2, 0.5, and 1.0. Single crystalline Czochralski grown p-type boron doped, (1 0 0) oriented silicon slides were used as substrates. The hydrosilylation grafting was performed according to two different procedures. The first procedure was reported in Ref. [37]. Briefly, 10 ml of alkene solution was placed in a small, three-necked flask fitted with a nitrogen inlet and a condenser. The solution was deoxygenated with dry nitrogen for at least 1 h. Subsequently, the silicon substrate was treated in a piranha solution for 12 min, rinsed in water for 2 min and etched in 1.0% hydrofluoric acid for 90 s and immediately placed in the solution. The solution was then refluxed at 200 °C for 2 h, under slow N_2 bubbling to prevent bumping. After cooling to room temperature, the sample was removed from the solution and cleaned by an ultrasonic cleaner in dichloromethane for 10 min. The second procedure followed the method described by Strother et al. [38]. Briefly, 2 mL of alkene solution was placed in a chamber with a quartz window and was deoxygenated by stirring in a dry box for at least 1 h. Subsequently, a Si(1 0 0) substrate, after the above described etching process, was immediately placed in the solution. The chamber remained under UV irradiation (254 nm) for 2 h. The sample was then removed from the solution and sonicated in dichloromethane for 10 min.

10-Undecylenic acid was obtained by hydrolysis of the 10-undecylenic acid methyl ester by two different procedures. Acid hydrolysis was performed in boiling acidified water (100 mM H_2SO_4) for 30 min, according to a modification of the method reported by Sieval et al. [35a]. Alkaline hydrolysis was performed by treatment with potassium *tert*-butoxide in DMSO according to a method reported by Strother et al. [38]. Grafted surfaces were dipped in a 250 mM solution of potassium *tert*-butoxide in DMSO for 30 s at room temperature followed by rinsing in acidified water (100 mM HCl).

Vapor phase anchoring of $Ni(acac)_2$ was performed in a low pressure (10^{-2} mTorr), horizontal reactor consisting of a quartz tube (i.d. 2.5 cm) with a total length of 15 cm. $Ni(acac)_2$ (Aldrich Chemical Co., 95%) was sublimated at 90 °C under low pressure and transported in the gas phase toward functionalized Si(1 0 0) substrate kept in the 110–150 °C temperature range for 60 min. After deposition samples were sonicated in ethanol for 15 min before analysis.

The XPS spectra were performed with a PHI ESCA/SAM 5600 Multi technique spectrometer equipped with a monochromatized Al Kα X-ray source. The analyses were carried out at various photoelectron angles relative to the sample surface in the 10–80° range with an acceptance angle of ±7°. BE scale was calibrated by centering the adventitious/hydrocarbon carbon C 1s at 285.0 eV [39–42].

Infrared spectra of the monolayers were recorded on JASCO FTIR 430 equipped with a Harrick GATR germanium single reflection ATR accessory, collecting the spectra with 80 scans at 4 cm^{-1} resolution.

3. Results and discussion

3.1. Preparation on engineered Si(100) surfaces

Diluted monolayers suited for $Ni(acac)_2$ anchoring were prepared by a two step procedure (Scheme 1): (i) Si-grafting of mixtures of 10-undecylenic acid methyl ester diluted with 1-decene within different mole fractions: $\chi_{ester}(soln) = 0.0, 0.2, 0.5, 0.8, 1.0$; (ii) the hydrolysis of the carboxylic groups in order to form free –COOH groups able to bond the Ni complex.

Mixed monolayers of ester/decene were silicon grafted, adopting either a photochemical or a thermal approach (see Section 2). No relevant differences were found between the two approaches.

XPS and ATR-IRAS were used to study the engineered surface after each reaction step.

Discussion on the shape changes of the C 1s spectral regions after the grafting of ester/decene mixtures has been reported elsewhere [37]. Briefly, C 1s spectra of either pure or mixed grafted 10-undecylenic acid methyl ester consist of four main components centered at (i) 283.7 eV (the carbide Si*C* bond); (ii) 285.0 eV (the aliphatic backbone); (iii) 287.4 eV (the esteric methyl –O*C*H_3) and (iv) 289.5 eV (the O*C*=O carboxylic groups). The atomic fraction between the 289.5 eV and 287.4 eV carbon components are always 1:1, as expected for the grafted ester [43]. A further component is also present at 286.0 eV, due to slightly oxidized carbon surface contaminants. As regards the C 1s spectra of grafted 1-decene, they consist of only two main components centered at 283.7 eV related to the carbide SiC bond, and at 285.0 eV due to the aliphatic backbone. A band is present at 286 eV, related to slightly oxidized carbon surface contaminants [44,45]. This feature is apparent in all the recorded spectra and it is likely due to the chemical manipulations.

The hydrolysis of the methyl ester was performed according to two procedures (acid and alkaline hydrolyses) as described in Section 2.

Fig. 1 compares C 1s spectra of samples grafted with pure 10-undecylenic methyl ester, before hydrolysis and either after acid catalyzed hydrolysis or after alkaline catalyzed hydrolysis.

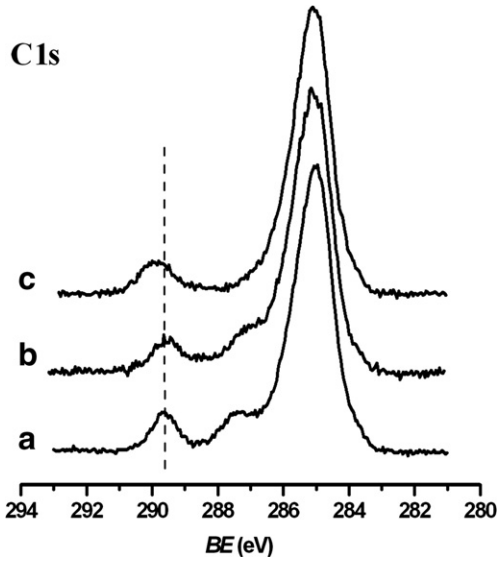

Fig. 1. High resolution C 1s XPS spectral region of (a) Si(100) substrate after grafting of the pure 10-undecylenic acid methyl ester; (b) ester decorated Si(100) substrate after acid catalyzed hydrolysis and (c) ester decorated Si(100) substrate after alkaline catalyzed hydrolysis.

C 1s spectra of samples obtained after acid hydrolysis are similar to those of the corresponding ester, but the esteric methyl –O*C*H_3 component (287.4 eV) is reduced, thus accounting for the occurrence of a partial hydrolysis of the esteric groups.

More evident changes occurred in the C 1s photoelectron spectral region after the alkaline hydrolysis. As matter of the fact, the esteric methyl –O*C*H_3 component (287.4 eV) disappears, thus indicating that the hydrolysis is almost complete. Note, in addition, that the C 1s component due to the carboxylic groups (at 289.5 eV in the ester) is shifted to BE = 289.8 eV (+0.3 eV) in the acid, consistent with a monolayer mainly terminated with free –COOH [46]. It is evident that alkaline hydrolysis is more efficient since after 30 s of alkaline treatment the methyl component –O*C*H_3 at 287.4 eV is lower than the same component after 30 min of acid treatment.

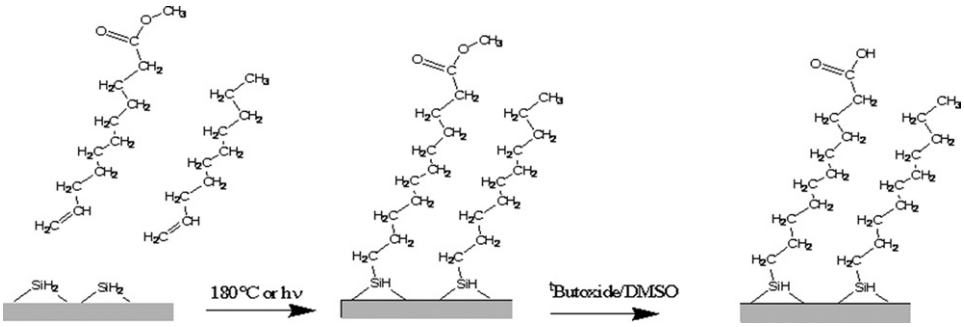

Scheme 1. Two step procedure for the preparation on engineered Si(100) surfaces.

BE and the relative contribution (f_x^C) of each carbon component to the total intensities of the C 1s region for the 10-undecylenic acid methyl ester and the sample after hydrolysis are summarized in Table 1.

The relative contribution (%) f_x^C can be obtained from the following equation: $f_x^C = \frac{I_x^C}{I^C} \times 100$ where x represents a particular C 1s component, I^C is the total spectral intensity and I_x^C denotes the intensity of the particular x component.

Mixed acid/decene monolayers obtained from various ester/decene grafting solutions show similar band components but different values of the relative contribution f_x^C. The relative contribution of C 1s components for mixed monolayer obtained for $\chi_{ester}(soln) = 0.0, 0.2, 0.5, 1.0$ after alkaline hydrolysis are reported in Table 2.

Note that $f_{289.8}^C$ is an indicator of the surface acid fraction $\chi_{acid}(surf)$ once normalized to homologue value of the pure acid surface (obtained for $\chi_{ester}(soln) = 1.0$). Data show clearly that the surface fraction of COOH groups directly depends on $\chi_{ester}(soln)$.

The photoelectron Si 2p region is a reliable indicator of the monolayer quality since it allows the evaluation of the substrate passivation against oxidation and, therefore, of the monolayer packing. The Si 2p region of freshly HF etched Si(1 0 0) consists of well resolved Si $2p_{3/2-1/2}$ spin–orbit doublets of the elemental silicon, no band around 103 eV (due to fully oxidized silicon) is detected [47]. Features due to Si 2p spectra after the grafting of mixed monolayers do not show sizeable surface oxidation, thus confirming the efficient passivation effects of the monolayer despite the oxidizing environments.

Angle resolved X-ray photoelectron spectroscopy was used to estimate the thickness of the grafted layers. Fig. 2 shows the angular dependence of the I^C/I^{Si} intensity ratios (I^C and I^{Si} are the total intensities of carbon and silicon, respectively) calculated for pure ester and pure decene monolayers.

In both cases, the I^C/I^{Si} ratios exponentially decrease with the electron take-off angle from the sample surface (θ), consistent with the presence of a carbonaceous overlayer on Si.

The intensity of XPS signals due to the silicon substrate covered by an overlayer of thickness d and that due to the overlayer itself are, respectively [48]:

$$I^{Si} = I_\infty^{Si} e^{\frac{-d}{\lambda_{Si\,2p}^C \operatorname{sen}\theta}} \quad (1)$$

and

$$I^C = I_\infty^C \left(1 - e^{\frac{-d}{\lambda_{C\,1s}^C \operatorname{sen}\theta}}\right) \quad (2)$$

Combining Eqs. (1) and (2), the I^C/I^{Si} intensity ratio is

$$\frac{I^C}{I^{Si}} = \frac{I_\infty^C \left(1 - e^{\frac{-d}{\lambda_{C\,1s}^C \operatorname{sen}\theta}}\right)}{I_\infty^{Si} e^{\frac{-d}{\lambda_{Si\,2p}^C \operatorname{sen}\theta}}} \quad (3)$$

where $\lambda_{Si\,2p}^C$ and $\lambda_{C\,1s}^C$ are the mean free paths of Si 2p and C 1s photoelectrons in a carbonaceous overlayer (4.15 and 3.6 nm, respectively [49]). I_∞^{Si} and I_∞^C are the intensities of pure Si and C elements on the same instrument and setting.

Given these positions, Eq. (3) can be adopted to reproduce experimental data in Fig. 2 as well as to provide an estimate of the thickness of the grafted film of about 1.25 and 1.3 nm for decene and ester, respectively. These values are consistent with the presence of grafted monolayers on the silicon surfaces.

3.2. Vapor phase deposition of nickel

Deposition was performed in the 100–150 °C temperature range at low pressure (10^{-2} mTorr) on grafted substrates. After each deposition samples were sonicated in ethanol to avoid the presence of weakly physisorbed complexes. For deposition below 150 °C, the absence of any signal around 103 eV indicates that no sizeable oxidation was present. Higher temperature of deposition induces the oxidation of the organic monolayer.

In order to evaluate the role of the engineered silicon, depositions were performed simultaneously on substrates with different COOH surface fractions (obtained for $\chi_{ester}(soln) = 0, 0.2, 0.5, 1.0$).

The amount of Ni deposited on the different substrates was evaluated by XPS analysis.

Fig. 3 reports the intensity ratio (I^{Ni}/I^{Si}) between the Ni $2p_{3/2}$ and Si 2p features as a function of the surface concentration of carboxylic groups (obtained from various ester mole fractions in the grafting solution). From Fig. 3 it is evident that the amount of anchored Ni directly depends on the surface COOH fraction.

Depositions on pure 1-decene decorated substrates results with a negligible amount of $Ni(acac)_2$, likely physisorbed on the hydrocarbon. By contrast, depositions on

Table 1
BE and the relative contribution (f_x^C) of carbon components to the total intensities of C 1s region for the Si(1 0 0) substrate grafted with 10-undecylenic acid methyl ester and the ester grafted Si(1 0 0) after either acid or alkaline hydrolysis

	C 1s components				
	OC=O BE (f_x^c)	H_3CO BE (f_x^c)	$CO_{contamin.}$ BE (f_x^c)	$C_{aliphatic}$ BE (f_x^c)	CSi BE (f_x^c)
Pure 10-undecylenic acid methyl ester	289.5 (7.4)	287.5 (7.4)	286.0 (18.5)	285.0 (64.5)	283.7 (2.1)
10-Undecylenic acid (acid hydrolysis)	289.5 (7.8)	287.4 (4.9)	286.1 (20.6)	285.0 (65.2)	283.6 (1.5)
10-Undecylenic acid (alkaline hydrolysis)	289.8 (6.8)	287.4 (1.3)	286.0 (16.2)	285.0 (74.3)	283.7 (1.3)
After $Ni(acac)_2$ deposition	288.9 (8.5)	287.0 (7.5)	286.0 (11.2)	285.0 (70.9)	283.7 (1.4)

Table 2
Relative contribution f_x^C of C 1s components and surface acid fraction χ_{acid}(surf) for various mixed monolayers

χ_{ester}(soln)	C 1s components					χ_{acid}(surf)
	$f^C_{289.8}$	$f^C_{287.4}$	$f^C_{286.0}$	$f^C_{285.0}$	$f^C_{283.7}$	
0.0	0.0	0.0	16.4	77.6	6.0	0.0
0.2	2.9	1.1	10.6	83.2	2.2	0.4
0.5	4.1	1.1	14.6	78.5	1.7	0.6
1.0	6.8	1.3	16.2	74.3	1.3	1.0

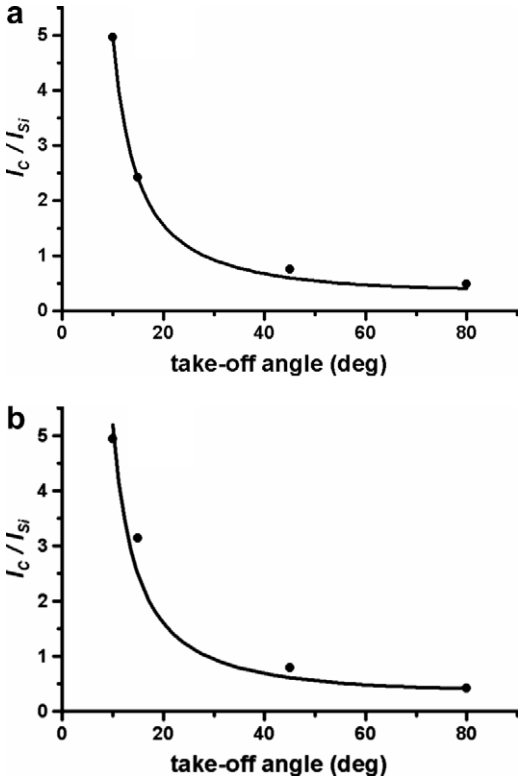

Fig. 2. Angular dependence of the I^C/I^{Si} intensity ratios for pure ester and pure decene monolayers. Solid lines are the best fit obtained with Eq. (3).

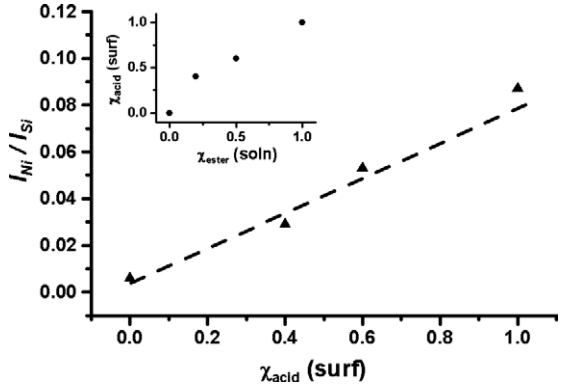

Fig. 3. The I^{Ni}/I^{Si} intensity ratio vs the surface mole fraction of 10-undecylenic acid, χ_{acid}(surf). In the box: the acid surface mole fractions vs the mole fraction of 10-undecylenic acid methyl ester in the binary precursor deposition solutions.

mixed 10-undecylenic acid/1-decene layers lead to relevant anchoring of Ni-containing material, the amount of which increases with COOH surface fraction.

The nature of the anchored Ni was investigated by high resolution XPS analysis.

A preliminary XPS spectrum was performed on $Ni(acac)_2$ powder in order to have a reference (Fig. 4a). The overall shape of the Ni region can be divided into edges split by spin–orbit coupling, referred to as $2p_{1/2}$ (≈890–870 eV) and $2p_{3/2}$ (≈870–862 eV) ranges, respectively [50–53]. XPS Ni $2p_{1/2}$ and $2p_{3/2}$ peaks appear at 873.8 and 856.1 eV, respectively. Two main satellite structures are present in both the $2p_{1/2}$ and $2p_{3/2}$ edges. They appear at the 2.3 and 4.9 eV high binding energy side of the main line in agreement with literature [50–53]. Above the 4.8 eV satellite, a shake-up type peak is present at 864.3 eV, typically observed for Ni(II) complexes. A shoulder is also present at 853.3 eV due to nickel oxide NiO contamination [54,55]. C 1s spectra (Fig. 4a) consist of two main components centered at (i) 285.0 eV (C–C bond and carbon adventitious) and (ii) 286.8 eV (C═O bond).

$Ni(acac)_2$ vapor phase deposition on mixed 10-undecylenic acid/1-decene layers leads to the amount of anchored Ni-containing material increasing with the fraction of COOH functionalities. In this context it is noted that despite the different acid/decene ratios, similar shapes are observed for Ni 2p and C 1s spectra.

The shape of the Ni 2p spectral region (Fig. 4b) on deposited films presents some notable differences compared to $Ni(acac)_2$ powder. XPS Ni $2p_{1/2}$ and $2p_{3/2}$ peaks appear at 874.4 and 856.8 eV, respectively. Two main satellite structures in the $2p_{3/2}$ region are still present at the 2.1 and 4.7 eV high binding energy side of the main $2p_{3/2}$ peak. These chemical shifts observed for the Ni complex are smaller than those previously observed for $Ni(acac)_2$ powders. This result indicates the chemisorption of the Ni complex. A shoulder is observed at 854.1 eV, indicating the presence of trace of Ni oxide contaminations.

The C 1s spectral region of samples grafted with mixed 10-undecylenic acid/1-decene monolayers shows a clear shift of the carbon feature toward lower binding energies (288.9 eV) indicating the presence of carboxylate COO^- groups [56]. However, this band, having a full width at half-maximum (fwhm) of 1.55 eV, is significantly broader than the correspondent band of the acid (fwhm = 1.2 eV) suggesting that contributions due to more than one component (i.e. COOH and COO^-) are involved. Moreover, a new band appears at 287.0 eV that can be related to the two carbonyls of the β-diketonate ligand, which, therefore, remains, partially bonded to the surface. These results indicate the chemisorption of nickel β-diketonate with the formation of an interfacial compound between the grafted carboxylate and the nickel β-diketonate. Note that the intensity ratio between the two components at 288.9 and 287.0 eV is about 1:1 (Table 1), thus indicating the presence of two carboxylic\carboxylate ligands for each β-diketonate ligand. The atomic ratio between Ni

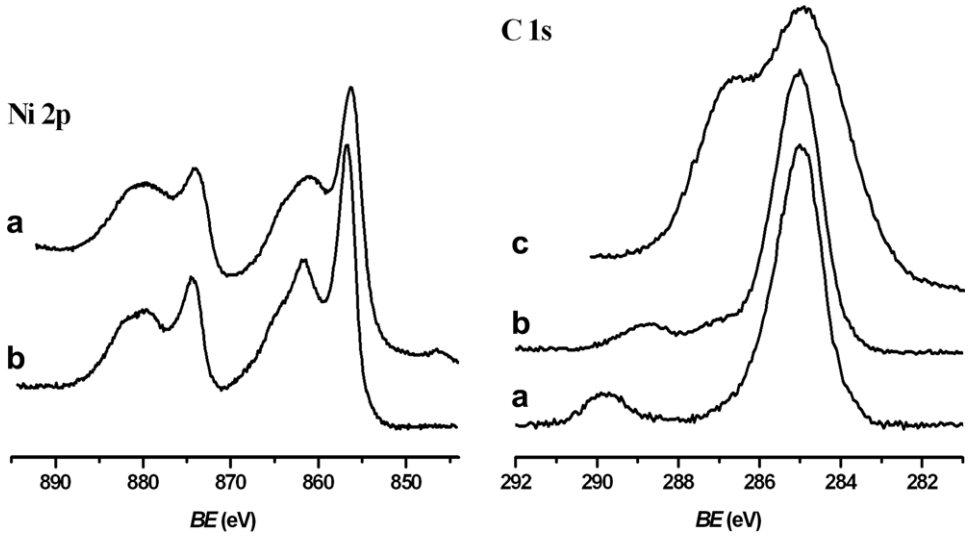

Fig. 4. Left: high resolution Ni 2p XPS spectral region of (a) $Ni(acac)_2$ commercial powders; (b) 10-undecylenic acid decorated Si(100) substrate after $Ni(acac)_2$ vapor phase anchoring. Right: high resolution C 1s XPS spectral region of (a) $Ni(acac)_2$ commercial powders; (b) 10-undecylenic acid decorated Si(100) substrate after $Ni(acac)_2$ vapor phase anchoring; (c) 10-undecylenic acid decorated Si(100) substrate.

and the mentioned components $C_{288.9}$ and $C_{287.0}$ inferred from the Ni $2p_{3/3}$ and C 1s signal evaluated by using Wagner sensitivity factors [57] is $Ni:C_{288.9}:C_{287.0} \sim 1:2:1.7$, thus suggesting the presence of one acac and two carboxylic/carboxylate ligands for each Ni atom. These results can be explained assuming that the $Ni(acac)_2$ chemisorption involves the substitution of one acac ligand with a carboxylate group on the surface. However, due to the steric hindrance of the anchored complexes, it is probable that many carboxylic groups remain unreacted, thus leading to the above mentioned 2:1 ratio between the grafted carboxylic/carboxylate and the acac ligands. A schematic summary of the deposition process is shown in Scheme 2.

Further insights into the structure of the grafted molecules were obtained by angular resolved XPS. Fig. 5 shows the angular dependence of the I^C/I^{Si}, I^{Ni}/I^{Si} and I^{Ni}/I^C intensity ratios (I^{Ni} is the total intensity of Ni $2p_{3/3}$ signal) calculated for a pure 10-uncylenic acid treated with $Ni(acac)_2$.

From Fig. 5 it is evident that both I^C/I^{Si} and I^{Ni}/I^{Si} exponentially decrease with θ, consistent with the presence of a Ni-containing carbonaceous overlayer on Si. On the other hand, the I^{Ni}/I^C ratio does not show an evident angular dependence even though it slightly increases with θ. This observation indicates that no Ni overlayer was formed on the grafted undecylenic acid, but the Ni is included in the carbonaceous layer. In addition, an attempt to fit the experimental points with (Eq. (3)) failed, thus indicating that the simplified model of a homogeneous carbonaceous overlayer on the Si substrate is no longer appropriate [48]. Assuming that after $Ni(acac)_2$ deposition the substrate coverage is no longer homogeneous and island formation occurs it is possible to modify Eq. (3) to account for a fractional overlayer [48]:

$$\frac{I^C}{I^{Si}} = \frac{I^C_\infty}{I^{Si}_\infty} \frac{\alpha\left(1 - e^{\frac{-d}{\lambda^C_{C\,1s}\,\mathrm{sen}\theta}}\right)}{1 - \alpha\left(1 - e^{\frac{-d}{\lambda^C_{Si\,2p}\,\mathrm{sen}\theta}}\right)} \tag{4}$$

where α is the fractional coverage of the substrate. Although this model is still oversimplified, it is useful to estimate the changes of thickness after β-diketonate anchoring. From the fit of experimental data, the fractional coverage and the estimated thickness are 0.8 and 2.3 nm, respectively. As expected, the thickness value is higher than 1.3 nm obtained for the ester monolayer before Ni β-diketonate deposition and, although overestimated, it is consistent with the presence of anchored molecules.

XPS characterization is also supported by ATR-IRAS results. Fig. 6 shows ATR-IRAS spectra of a sample grafted with 10-undecylenic acid before and after $Ni(acac)_2$ anchoring. ATR-IRAS spectrum of $Ni(acac)_2$ (powders in KBr) is used as reference. Two spectral regions are reported in Fig. 6 since they are diagnostic for the grafted layers, namely that of CH stretching between 3000 and 2700 cm^{-1} and that between 1800 and 1200 cm^{-1} for the stretchings of carbonyl/carboxyl functional groups. The grafted acid (Fig. 5a) shows the expected bands at 2926 cm^{-1} and 2854 cm^{-1} assigned to the $\nu_a(CH_2)$ and $\nu_s(CH_2)$ stretching modes, respectively. The characteristic stretches centered at 1740 cm^{-1} are clearly visible [56]. After the Ni β-diketonate anchoring, the spectra became more intense accounting for the increased amount of anchored material. The sample shows similar bands to the untreated acid due to the $\nu_a(CH_2)$ and $\nu_s(CH_2)$ stretching modes. A new feature at 2960 cm^{-1} is observed due to the CH_3 asymmetric in-plane CH stretching mode due to the acac ligands. In addition, typical features around 1598, 1524, 1460, and 1404 cm^{-1} are present due to the

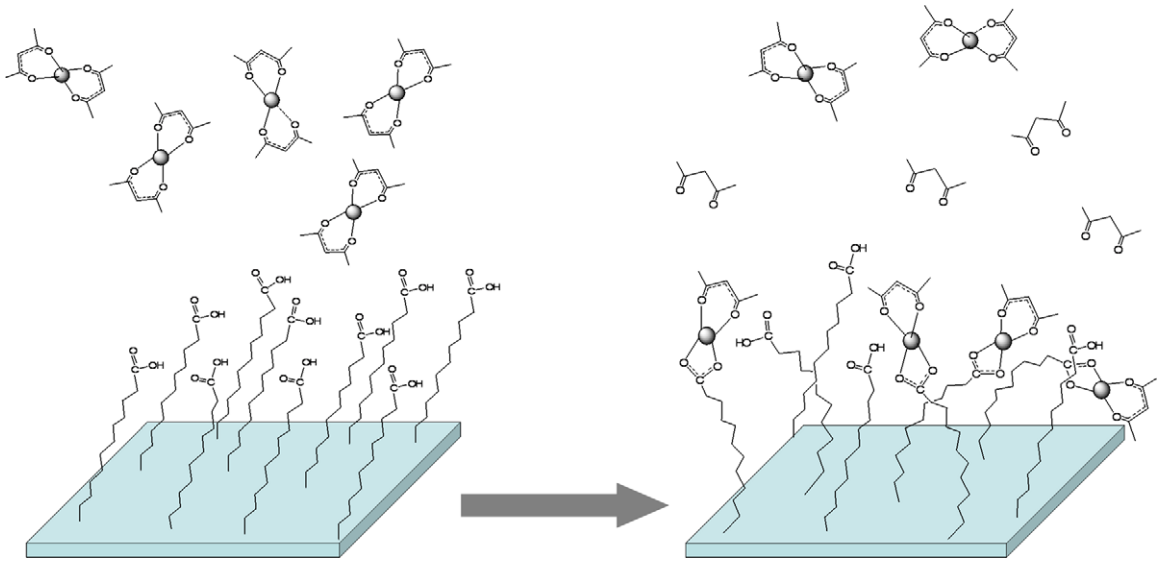

Scheme 2. Schematic summary of the $Ni(acac)_2$ vapor phase anchoring.

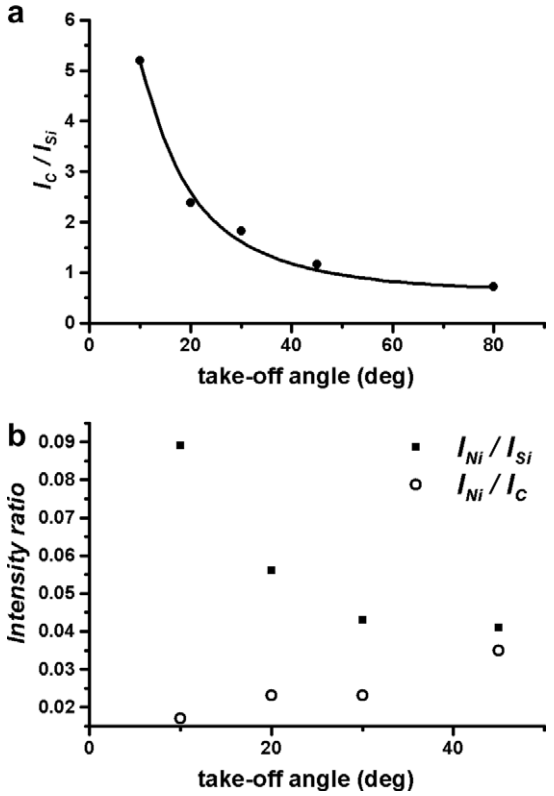

Fig. 5. Angular dependence of (a) I^C/I^{Si} and (b) I^{Ni}/I^{Si} and I^{Ni}/I^C intensity ratios for pure 10-undecylenic acid decorated Si(100) substrate after $Ni(acac)_2$ vapor phase anchoring. Solid lines are the best fit obtained with Eq. (4).

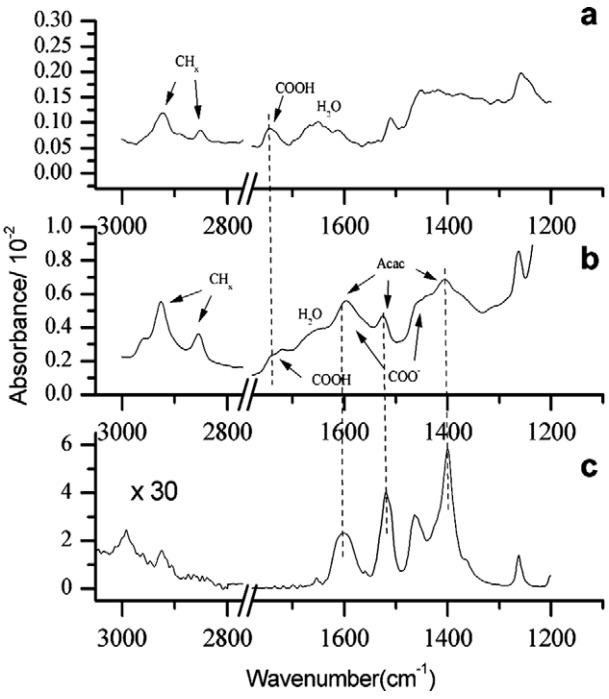

Fig. 6. ATR-IRAS spectra of (a) 10-undecylenic acid decorated Si(100) substrate; (b) 10-undecylenic acid decorated Si(100) substrate after $Ni(acac)_2$ vapor phase anchoring; (c) $Ni(acac)_2$ commercial powders in KBr.

coordinated acac. The bands at 1598 and 1524 cm^{-1} are assigned to the combination of ν(C=O) and ν(C=C) stretches, the other two features at 1460 and 1404 cm^{-1} are assigned to the δ(CH) + ν(C=C) and $\delta(CH_3)$ vibration, respectively [58].

Bands at 1598 cm^{-1} and at 1460 cm^{-1} are broader than the $Ni(acac)_2$ reference, likely due to the carboxylate bands around 1570 and 1450 cm^{-1} [56]. According to XPS results, the stretches at 1740–1700 cm^{-1} due to unreacted carboxylic groups are still present, even though significantly reduced. A broad band in the 1660–1620 cm^{-1} range due to adsorbed water was present in both spectra.

4. Conclusions

This study has shown a viable route for the anchoring of Ni β-diketonates on Si(100), which is a surface suited to integration with well-established silicon technologies. The strategy is based on the preparation of engineered Si surfaces with a 10-undecylenic acid monolayer. XPS and ATR-IRAS measurements have suggested that the anchoring path involves the substitution of an acac ligand with a carboxylate group of the grafted monolayer. In addition, it has proven possible to control the surface density of the Ni-containing complex by tuning the surface concentration of the grafting carboxylate groups. XPS data show that the surface concentration χ_{acid}(surf) of the grafting methyl 10-undecylenate depends on the mole fraction χ_{ester}(soln) of the precursor binary solution with the 10-decene spectator. XPS results after Ni β-diketonate anchoring show that the Ni/Si intensity ratio increases parallel to the ester mole fraction in solution and, hence, to the surface concentration χ_{acid}(surf). This bottom-up approach represents a promising perspective for controlled modification of substrates of technological importance.

Acknowledgments

The authors thank the Ministero Istruzione Università e Ricerca (MIUR, Roma) for financial support (PRIN 2005 and FIRB 2003 projects).

References

[1] C.A. Mirkin, M.A. Ratner, Annu. Rev. Phys. Chem. 43 (1992) 719.
[2] A.J. Ricco, R.M. Crooks, G.C. Osbourn, Acc. Chem. Res. 31 (1998) 289.
[3] R. Paolesse, C. Dinatale, A. Macagnano, F. Davide, T. Boschi, A. Damico, Sens. Actuators, B 47 (1998) 70.
[4] D.S. Everhart, Chemtech 4 (1999) 30.
[5] T. Wessa, W. Goepel, Fresenius, J. Anal. Chem. 361 (1998) 239.
[6] S. Storri, T. Santoni, M. Minunni, M. Mascini, Biosens. Bioelectron. 13 (1998) 347.
[7] D.L. Allara, Biosens. Bioelectron. 10 (1995) 771.
[8] A. Ulman, An Introduction to Ultrathin Organic Films: From Langmuir–Blodgett to Self-Assembly, Academic, New York, 1991.
[9] D. Pawlowski, B. Tieke, Langmuir 19 (2003) 6498.
[10] J.H. Clark, D. Macquarrie, J. Chem. Soc. Rev. 25 (1996) 303.
[11] J. Wang, ACS Symp. Ser. 487 (1992) 125.
[12] J.C. Gabriel, S. Voccia, C. Detrembleur, M. Ignatova, R. Gouttebaron, R. Jerome, Chem. Commun. (2003) 2500.
[13] R. Tannenbaum, C. Hakanson, A. Zeno, M. Tirrell, Langmuir 18 (2002) 5592.
[14] W.Q. Han, S.S. Fan, Q.Q. Li, Y.D. Hu, Science 277 (1997) 1287.
[15] A. Godwin, M. Hartenstein, A.H.E. Muller, S. Brocchini, Angew. Chem., Int. Ed. 40 (2001) 549.
[16] Y.G. Slizhov, M.A. Gavrilenko, Russ. J. Coord. Chem. 28 (2002) 736.
[17] I.V. Babich, Y.V. Plyuto, A.D. Van Langeveld, J.A. Moulijn, Appl. Surf. Sci. 115 (1997) 267.
[18] J.C. Kenvin, M.G. White, M.B. Mitchel, Langmuir 7 (1991) 1198.
[19] J.A.R. Van Veen, P.C. De Jong-Versloot, G.M.M. Van Kessel, F.J. Fels, Thermochim. Acta 152 (1989) 359.
[20] J.A.R. Van Veen, G. Jonkers, W.H. Hesselink, J. Chem Soc. Faraday Trans. I 85 (1989) 389.
[21] L.P. Lindfors, S. Smeds, Catal. Lett. 28 (1994) 291.
[22] S. Ferretti, S. Paynter, D.A. Russell, K.E. Sapsford, D.J. Richardson, TrAC, Trends Anal. Chem. 19 (2000) 530.
[23] M. Mrksich, Chem. Soc. Rev. 29 (2000) 267.
[24] E. Ostuni, L. Yan, G.M. Whitesides, Colloids Surf. B 15 (1999) 3.
[25] H. Schonherr, V. Chechik, C.J.M. Stirling, G.J. Vancso, J. Am. Chem. Soc. 122 (2000) 3679.
[26] H. Schonherr, V. Chechik, C.J.M. Stirling, G.J. Vancso, ACS Symp. Ser. 781 (2001) 36.
[27] B. Dordi, H. Schönherr, G.J. Vancso, Langmuir 19 (2003) 5780.
[28] O. Prucker, J. Rühe, Macromolecules 31 (1998) 592.
[29] S. Hermes, F. Schröder, R. Chelmowski, C. Wöll, R.A. Fischer, J. Am. Chem. Soc. 127 (2005) 13744.
[30] C. Duschl, M. Liley, H. Vogel, Angew. Chem., Int. Ed. Engl. 33 (1994) 1274.
[31] J. Weib, H.J. Himmel, R.A. Fischer, C. Woll, Chem. Vap. Deposition 4 (1998) 17.
[32] A. Dube, A.R. Chadeayne, M. Sharma, P.T. Wolczanski, J.R. Engstrom, J. Am. Chem. Soc. 127 (2005) 14299.
[33] A.S. Killampalli, P.F. Ma, J.R. Engstrom, J. Am. Chem. Soc. 127 (2005) 6300.
[34] G.F. Cerofolini, G. Ferla, J. Nanopart. Res. 4 (2002) 185.
[35] (a) A.B. Sieval, A.L. Demirel, J.M. Nissink, M.R. Linford, J.H. van der Maas, W.H. de Jeu, H. Zuilhof, E.J.R. Sudhölter, Langmuir 14 (1998) 1759;
(b) G.F. Cerofolini, C. Galati, S. Reina, L. Renna, G.G. Condorelli, I.L. Fragalà, G. Giorgi, A. Sgamellotti, N. Re, Appl. Surf. Sci. 246 (2005) 52;
(c) Q.-Y. Sun, L.C.P.M. de Smet, B. van Lagen, M. Giesbers, P.C. Thune, J. van Engelenburg, F.A. de Wolf, H. Zuilhof, E.J.R. Sudholter, J. Am. Chem. Soc. 127 (2005) 2514.
[36] (a) J. Terry, M.R. Linford, C. Wigren, R. Cao, P. Pianetta, C.E.D. Chidsey, Appl. Phys. Lett. 71 (1997) 1056;
(b) M.M. Sung, G.J. Kluth, O.K. Yauw, R. Maboudian, Langmuir 13 (1997) 6164.
[37] (a) G.G. Condorelli, A. Motta, I.L. Fragalà, F. Giannazzo, V. Ranieri, A. Caneschi, D. Gatteschi, Angew. Chem., Int. Ed. 43 (2004) 4081;
(b) G.G. Condorelli, A. Motta, M. Favazza, P. Nativo, I.L. Fragalà, D. Gatteschi, Chem. Eur. J. 12 (2006) 2558.
[38] T. Strother, W. Cai, X. Zhao, R.J. Hamers, L.M. Smith, J. Am. Chem. Soc. 122 (2000) 1205.
[39] D. Briggs, G. Beamson, Anal. Chem. 64 (1992) 1729.
[40] I.L. Swift, Surf. Interface Anal. 4 (1982) 47.
[41] G.F. Cerofolini, C. Galati, S. Lorenti, L. Renna, O. Viscuso, C. Bongiorno, V. Raineri, C. Spinella, G.G. Condorelli, I.L. Fragalà, A. Terrasi, Appl. Phys. A 77 (2003) 403.
[42] D. Briggs, second ed., in: D. Briggs, M.P. Seah (Eds.), Practical Surfaces Analysis, vol. 1, WILEY-VCH, Weinheim, Germany, 1995, p. 440.
[43] D. Briggs, G. Beamson, Anal. Chem. 65 (1993) 5151.
[44] H. Jin, C.R. Kinser, P.A. Bertin, D.E. Kramer, J.A. Libera, M.C. Hersam, S.T. Nguyen, M.J. Bedzyk, Langmuir 20 (2004) 6252.
[45] F. Cecchet, P. Rudolf, S. Rapino, M. Margotti, F. Paolucci, J. Baggerman, A.M. Brouwer, E.R. Kay, J.K.Y. Wong, D.A. Leigh, J. Phys. Chem. B. 108 (2004) 15192.
[46] N. Betz, S. Dapoz, M.J. Guittet, Nucl. Instrum. Methods Phys. Res. B 131 (1997) 252.
[47] G.F. Cerofolini, C. Galati, L. Renna, O. Viscuso, M. Camalleri, S. Lorenti, G.G. Condorelli, I.L. Fragalà, Appl. Phys. 35 (2002) 1032.
[48] D. Briggs, second ed., in: D. Briggs, M.P. Seah (Eds.), Practical Surfaces Analysis, vol. 1, WILEY-VCH, Weinheim, Germany, 1995, p. 244.
[49] C.D. Bain, G.M. Whitesides, J. Phys. Chem. 93 (1989) 1670.
[50] C.A. Tolmann, W.M. Riggs, W.J. Linn, C.M. King, R.C. Wendt, Inorg. Chem. 12 (1973) 2770.
[51] M.O. De Souza, F.M.T. Mendes, R.F. De Souza, J.H.Z. Dos Santos, Micropor. Mesopor. Mater. 69 (2004) 217.

[52] J.S.H.Q. Pereira, D.C. Frost, C.A. McDowell, J. Chem. Phys. 72 (1980) 5151.
[53] G.C. Herdt, A.W. Czanderma, J. Vac. Sci. Technol. A 17 (1999) 3415.
[54] D. Alders, F.C. Voogt, T. Hibma, G.A. Sawatzky, Phys. Rev. B 54 (1996) 7716.
[55] V. Biju, M.A. Khadar, J. Nano. Res. 4 (2002) 247.
[56] T.M. Willey, A.L. Vance, T. van Buuren, C. Bostedt, A.J. Nelson, L.J. Terminello, C.S. Fadley, Langmuir 20 (2004) 2746.
[57] C.D. Wagner, L.E. Davis, M.V. Zeller, J.A. Taylor, R.H. Raymond, L.H. Gale, Surf. Interface Anal. 4 (1981) 211.
[58] K. Nakamoto, Infrared and Raman Spectra of Inorganic and Coordination Compounds, third ed., John Wiley & sons, New York, 1978.